JPE 16-2-20

http://dx.doi.org/10.6113/JPE.2016.16.2.598
ISSN(Print): 1598-2092 / ISSN(Online): 2093-4718

A Backstepping Control of LSM Drive Systems Using Adaptive Modified Recurrent Laguerre OPNNUO

Chih-Hong Lin†

†Department of Electrical Engineering, National United University, Miaoli, Taiwan

Abstract

The good control performance of permanent magnet linear synchronous motor (LSM) drive systems is difficult to achieve using linear controllers because of uncertainty effects, such as fictitious forces. A backstepping control system using adaptive modified recurrent Laguerre orthogonal polynomial neural network uncertainty observer (OPNNUO) is proposed to increase the robustness of LSM drive systems. First, a field-oriented mechanism is applied to formulate a dynamic equation for an LSM drive system. Second, a backstepping approach is proposed to control the motion of the LSM drive system. With the proposed backstepping control system, the mover position of the LSM drive achieves good transient control performance and robustness. As the LSM drive system is prone to nonlinear and time-varying uncertainties, an adaptive modified recurrent Laguerre OPNNUO is proposed to estimate lumped uncertainties and thereby enhance the robustness of the LSM drive system. The on-line parameter training methodology of the modified recurrent Laguerre OPNN is based on the Lyapunov stability theorem. Furthermore, two optimal learning rates of the modified recurrent Laguerre OPNN are derived to accelerate parameter convergence. Finally, the effectiveness of the proposed control system is verified by experimental results.

Key words: Backstepping control, Laguerre orthogonal polynomial neural network, Permanent magnet linear synchronous motor

I. INTRODUCTION

Permanent magnet linear synchronous motors (LSMs), which are direct-drive machines, have been widely used in industrial robots, semiconductor manufacturing systems, and machine tools [1]-[3] because of their high-performance servo-drive property.

A backstepping design involves the recursive selection of the appropriate functions of state variables as pseudo-control inputs for lower dimension subsystems of an overall system. Each backstepping stage results in a new pseudo-control design, which is expressed in terms of the pseudo control designs from the preceding design stages. The termination of the procedure results in a feedback design for true control inputs; this outcome achieves the original design objective by virtue of a final Lyapunov function, which is formed by summing up the Lyapunov functions associated with each individual design stage [4], [5]. Some existing methods use off-line data collected from machines under static conditions, which change during motor operation as a result of changes in motor parameters. Some methods use linear models of machines, which may not be suitable for high-performance applications with uncertainties. Neural networks (NNs) show great potential for modeling nonlinear systems, which is difficult to achieve using traditional techniques owing to the inherent parallel structure and learning ability of such systems. However, NNs feature static mapping. Moreover, the weight updates of NNs do not utilize the internal information of NNs, and function approximation is sensitive to training data. Recurrent NNs have received increasing attention because of their structural advantages in the modeling of nonlinear systems and their dynamic system control [6]-[10]. These networks are capable of effectively identifying and controlling complex process dynamics, but they entail considerable computational complexity. The recurrent Laguerre orthogonal polynomial NN [11]-[13]

Manuscript received Jul. 18, 2015; accepted Nov. 5, 2015
Recommended for publication by Associate Editor Shihua Li.
†Corresponding Author: jhlin@nuu.edu.tw
Tel: +886-3-7382464, Fax: +886-3-7382468, Nat'l United University
Department of Electrical Engineering, National United University, Taiwan

features dynamic mapping and demonstrates good control performance in the presence of uncertainties. Hence, the present study proposes a backstepping control system using adaptive modified recurrent Laguerre OPNNUO for LSM drive systems. The purpose of this study is to investigate and implement the proposed novel approach and thereby enhance system robustness.

This paper is organized as follows. The system structure of the LSM drive system is reviewed in Section II. A backstepping control design method using adaptive recurrent Laguerre OPNNUO is presented in Section III. The experimental results are illustrated in Section IV. The conclusions are given in Section V.

II. CONFIGURATION OF LSM DRIVE SYSTEM

The machine model of an LSM can be described in a synchronous rotating reference frame as follows [1]-[3]:

$$v_q = R_s i_q + \dot{\lambda}_q + \omega_e \lambda_d \tag{1}$$

$$v_d = R_s i_d + \dot{\lambda}_d - \omega_e \lambda_q \tag{2}$$

where

$$\lambda_q = L_q i_q \tag{3}$$

$$\lambda_d = L_d i_d + \lambda_{PM} \tag{4}$$

$$\omega_e = P\omega_r \tag{5}$$

and v_d, v_q are the d and q axis voltages, respectively; i_d, i_q are the d and q axis currents, respectively; R_s is the phase winding resistance; L_d, L_q are the d and q axis inductances, respectively; ω_r is the angular velocity of the mover; ω_e is the electrical angular velocity; λ_{PM} is the permanent magnet flux linkage; and P is the number of pole pairs. Moreover,

$$\omega_r = \pi v_r / \tau \tag{6}$$

$$v_e = P v_r = 2\tau f_e \tag{7}$$

where v_r is the linear velocity, τ is the pole pitch, v_e is the electric linear velocity, and f_e is the electric frequency. The developed electromagnetic power is given by [2]

$$P_e = F_e v_e = 3P[\lambda_d i_q + (L_d - L_q) i_d i_q]\omega_e / 2 \tag{8}$$

Thus, the electromagnetic force is

$$F_e = 3\pi P[\lambda_d i_q + (L_d - L_q) i_d i_q] / 2\tau \tag{9}$$

and the mover dynamic equation is

$$F_e = M\dot{v}_r + Dv_r + F_L \tag{10}$$

where F_e is the electromagnetic force, M is the total mass of the moving element system, D is the viscous friction and iron-loss coefficient, and F_L is the external disturbance term.

The basic control approach of an LSM servo drive is based on field orientation [2]. The flux position in the d–q coordinates can be determined with Hall sensors. In (4), (8), and (9), if $i_d = 0$, then the d-axis flux linkage λ_d is fixed because λ_{PM} is constant for an LSM. Moreover, the electromagnetic force F_e is proportional to i_q^*, which is determined by a closed-loop control. The rotor flux is only produced in the d-axis, whereas the current vector is generated in the q-axis for field-oriented control. As the generated motor force is linearly proportional to the q-axis current while the d-axis rotor flux is constant in (4), the maximum force per ampere can be achieved. The resulting force equation is

$$F_e = 3\pi\lambda_{PM} i_q / 2\tau \tag{11}$$

The configuration of a field-oriented LSM servo drive system is shown in Fig. 1, which consists of an LSM, a sinusoidal pulse-width-modulation (PWM)control modulator and current control, a field-orientation mechanism, a coordinate translator, a speed control loop, a position control loop, linear scale and Hall sensors, and three sets of isulated-gate bipolar transistor (IGBT) power modules inverter. The flux position of the permanent magnet is detected by the output signals of the Hall sensors denoted as U, V, and W. Iron disks of different sizes can be mounted on the mover of the LSM to change the mass of the moving element and viscous friction. The field-oriented mechanism drive system is implemented with an field-programmable gate array (FPGA) control system, and the control law is implemented with a digital signal processor (DSP) control system.

With the implementation of field-oriented control [1-3], the LSM drive can be simplified into a control system, the block diagram of which is shown in Fig. 2. That is,

$$F_e = K_f i_q^* \tag{12}$$

$$K_f = 3\pi P\lambda_{PM} / 2\tau \tag{13}$$

$$H_p(s) = \frac{1}{Ms + D} \tag{14}$$

where K_f is the thrust coefficient, i_q^* is the command of thrust current, and s is the Laplace's operator.

The LSM used in this study features the following: 220 V, 3.5 A, 1 kW, and 213 N. For a convenient controller design, the position and speed signals in the control loop are set to 1 V = 0.075 m and 1 V = 0.075 m/s, respectively. The parameters of the system are

$$\begin{aligned} K_f &= 60.8 \text{ N/A}, \\ \overline{M} &= 2.7\text{kg} = 0.2025 \text{ Nsec/V} \\ \overline{D} &= 92.56 \text{ kg/sec} = 6.942 \text{ N/V} \end{aligned} \tag{15}$$

The "$-$" symbol represents the system parameter in the

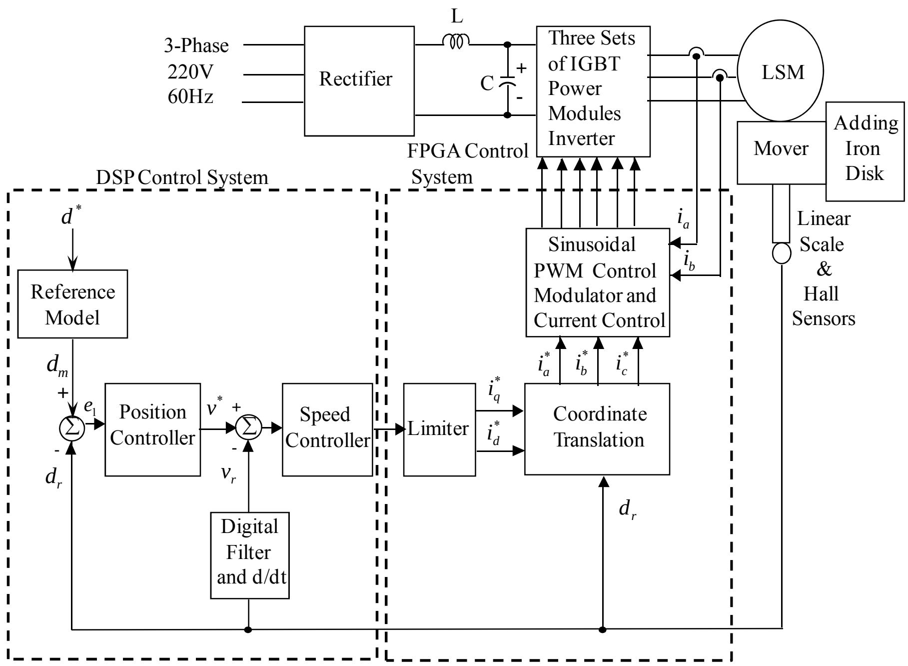

Fig. 1. Configuration of the LSM drive system.

nominal condition.

III. A BACKSTEPPING CONTROL SYSTEM DESIGN USING ADAPTIVE MODIFIED RECURRENT LAGUERRE OPNNUO

By considering an LSM servo drive system with parameter variations, external load disturbances, and friction forces, we can rewrite (10) as

$$\dot{d}_r = v_r = X_p \tag{16}$$

$$\dot{X}_p = (a_1 + \Delta a)X_p + (b_1 + \Delta b)u_a + c_1 F_L \tag{17}$$

$$Y = d_r \tag{18}$$

where d_r is the mover position of the LSM; X_p is the mover velocity of the LSM; $a_1 = -D/M$; $b_1 = K_f/M > 0$; $c_1 = -1/M$; Δa and Δb denote the uncertainties introduced by system parameters M and D, respectively; and u_a is the control input to the LSM drive system. By reformulating (17), the following can be derived:

$$\dot{X}_p = a_1 X_p + b_1 u_a + q \tag{19}$$

where q is the lumped uncertainty defined by

$$q \equiv \Delta a X_p + \Delta b u_a + c_1 F_L \tag{20}$$

The lumped uncertainty q is assessed by an adaptive uncertainty observer and is assumed to be constant during the observation. The above assumption is valid in the practical digital processing of the observer because the sampling period of the observer is short enough compared with the variation of q.

The control objective is to design a backstepping control system for the output Y of the system shown in (18) to asymptotically track the reference trajectory $Y_d(t)$, which is d_m. The proposed backstepping control system is designed to achieve the position-tracking objective. The step-by-step process is described as follows.

Step 1: For the position-tracking objective, the tracking error is defined as

$$z_1 = d_m - d_r = Y_d - Y \tag{21}$$

and its derivative is defined as

$$\dot{z}_1 = \dot{Y}_d - \dot{Y} = \dot{Y}_d - X_p \tag{22}$$

The following stabilizing function is defined:

$$\eta = k_1 z_1 + \dot{Y}_d + k_2 \sigma \tag{23}$$

where k_1 and k_2 are positive constants and $\sigma = \int z_1(\tau)d\tau$ is an integral action. We can ensure that the tracking error converges to zero using the integral action. Then, the first Lyapunov function L_1 is chosen as

$$L_1 = z_1^2 / 2 \tag{24}$$

The virtual tracking error $z_2 = X_p - \eta$ is defined. The derivative of L_1 is

$$\dot{L}_1 = z_1 \dot{z}_1 = z_1(\dot{Y}_d - z_2 - \eta) = -z_1 z_2 - k_1 z_1^2 - k_2 z_1 \sigma \tag{25}$$

Step 2: The derivative of z_2 is now expressed as

$$\begin{aligned} \dot{z}_2 &= \dot{X}_p - \dot{\eta} = a_1 X_p + b_1 u_a + q - \dot{\eta} \\ &= a_1(z_2 + \eta) + b_1 u_a + q - \dot{\eta} \end{aligned} \tag{26}$$

To design the backstepping control system, the lumped uncertainty q is assumed to be bounded, i.e., $|q| \le \bar{q}$. Then, the following Lyapunov function is defined as

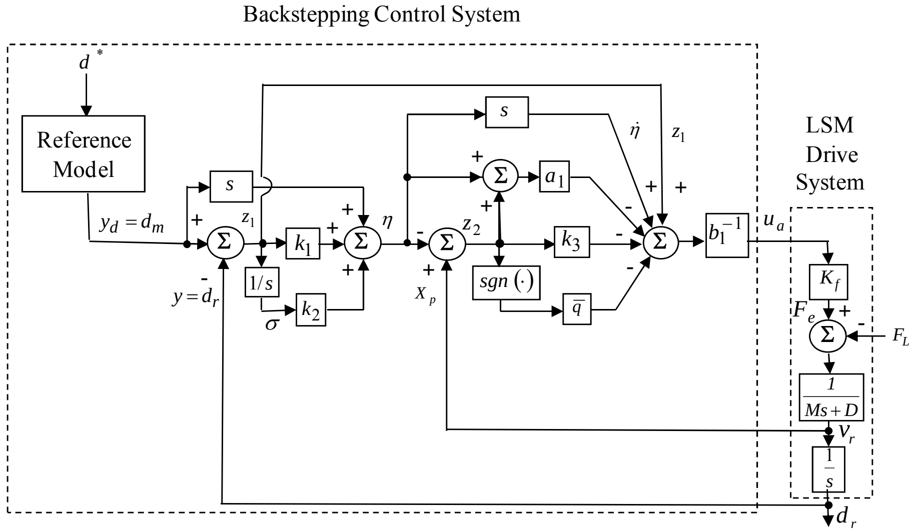

Fig. 2. Block diagram of the backstepping control system.

$$L_2 = L_1 + k_2\sigma^2/2 + z_2^2/2 \tag{27}$$

Using (25) and (26), the derivative of L_2 can be derived as follows:

$$\begin{aligned}\dot{L}_2 &= \dot{L}_1 + k_2\sigma\dot{\sigma} + z_2\dot{z}_2\\ &= -z_1z_2 - k_1z_1^2 - k_2z_1\sigma + k_2\sigma\dot{\sigma} + z_2[a_1(z_2+\eta) + b_1u_a + q - \dot{\eta}]\\ &= -k_1z_1^2 + z_2[-z_1 + a_1(z_2+\eta) + b_1u_a + q - \dot{\eta}]\end{aligned} \tag{28}$$

According to (28), the backstepping control law u_a can be designed as follows:

$$u_a = b_1^{-1}[z_1 - k_3z_2 - a_1(z_2+\eta) - \bar{q}sgn(z_2) + \dot{\eta}] \tag{29}$$

By substituting (29) into (28), (28) can be obtained as

$$\begin{aligned}\dot{L}_2 &= -k_1z_1^2 - k_3z_2^2 + z_2q - |z_2|\bar{q} \le -k_1z_1^2 - k_3z_2^2 - |z_2|(\bar{q} - |q|)\\ &\le -k_1z_1^2 - k_3z_2^2\end{aligned} \tag{30}$$

The following term is then defined:

$$\phi(t) = k_1z_1^2 + k_3z_2^2 \le -\dot{L}_2 \tag{31}$$

Then,

$$\int_0^t \phi(\tau)\,d\tau \le L_2(z_1(0), z_2(0)) - L_2(z_1(t), z_2(t)) \tag{32}$$

Given that $L_2(z_1(0), z_2(0))$ is bounded and that $L_2(z_1(t), z_2(t))$ is non-increasing and bounded, $\lim_{t\to\infty}\int_0^t \phi(\tau)\,d\tau < \infty$. Moreover, $\dot{\phi}(t)$ is bounded; thus, $\phi(t)$ is uniformly continuous [14], [15]. By using Barbalat's lemma [14], [15], $\lim_{t\to\infty}\phi(t) = 0$. That is, z_1 and z_2 converge to zero as $t\to\infty$. Moreover, $\lim_{t\to\infty} Y(t) = Y_d$, and $\lim_{t\to\infty} X_p = \dot{Y}_d$. Therefore, the backstepping control system is asymptotically stable. The stability of the backstepping control system (Fig. 2) can be guaranteed.

Step 3:

Given that the lumped uncertainty q is unknown in practical applications, the upper bound $\bar{q}$ is difficult to determine. Therefore, a modified recurrent Laguerre OPNNUO is proposed to adapt the value of the lumped uncertainty $\hat{q}$.

A three-layer modified recurrent Laguerre OPNN, which comprises an input layer (the i layer), a hidden layer (the j layer), and an output layer (the k layer), is adopted to implement the proposed control system.

$$y_i^1 = f_i^1\left(\prod_k x_i^1(N)w_{ik}^1 y_k^3(N-1)\right), \quad i = 1, 2 \tag{33}$$

$$y_j^2 = G_j\left(\sum_{i=1}^{2} y_i^1(N) + \beta\, y_j^2(N-1)\right), \ j = 0, 1, \cdots, m-1 \tag{34}$$

$$y_k^3 = f_k^3\left(\sum_{j=0}^{m-1} w_{kj}^2 y_j^2(N)\right), \quad k = 1 \tag{35}$$

$x_1^1 = d_m - d_r = z_1$ and $x_2^1 = z_1(1 - z^{-1}) = \Delta z_1$ are the tracking error and tracking error change, respectively. w_{ik}^1 and w_{kj}^2 are the recurrent weight between the output layer and the input layer and the connective weight between the hidden layer and the output layer, respectively. N denotes the number of iterations. The Laguerre orthogonal polynomial [11]-[13] $G_n(x)$ is the argument of the polynomials with $-1 < x < 1$; n is the order of expansion. m is the number of nodes. β is the self-connecting feedback gain of the hidden layer selected between 0 and 1. $G_0(x) = 1$, $G_1(x) = 1 - x$, and $G_2(x) = x^2 - 4x + 2$. The higher-order Laguerre orthogonal polynomials may be generated by the recursive formula $G_{h+1}(x) = [(2h+1-x)G_h(x) - hG_{h-1}(x)]/(h+1)$. f_i^1 and f_k^3 are the activation functions selected as linear functions. The recurrent modified Laguerre orthogonal polynomial NN output $y_k^3(N) = \hat{q}$ can be denoted as

$$y_k^3(N) = \hat{q}(\mathrm{o}) = \mathrm{o}^T\psi \tag{36}$$

where $\mathrm{o} = \left[w_{10}^2\ w_{11}^2 \cdots\cdots w_{1,m-1}^2\right]^T$ is the collection of adjustable parameters of the modified recurrent Laguerre

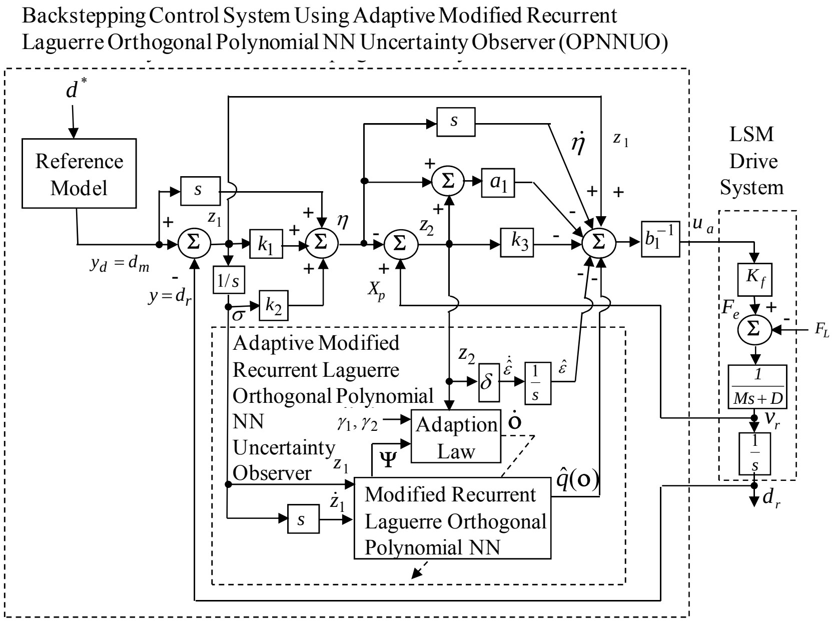

Fig. 3. Block diagram of the backstepping control system using adaptive modified recurrent Laguerre OPNNUO.

orthogonal polynomial NN. $\psi = \left[y_0^2 \; y_1^2 \cdots\cdots y_{m-1}^2\right]^T$, in which y_j^2 is determined by the selected Laguerre orthogonal polynomials and $0 \le y_j^2 \le 1$.

To develop the adaptation laws of the modified recurrent Laguerre OPNNUO u, the minimum reconstructed error ε is defined as follows:

$$\varepsilon = q - q(\mathrm{o}^*) \tag{37}$$

where o^* is an optimal weight vector that achieves the minimum reconstructed error. The absolute value of ε is assumed to be less than a small positive constant $\bar{\varepsilon}$ (i.e., $|\varepsilon| \le \bar{\varepsilon}$). Then, a Lyapunov candidate is chosen as

$$L_3 = L_2 + (\hat{\varepsilon} - \varepsilon)^2/(2\delta) + (\mathrm{o} - \mathrm{o}^*)^T(\mathrm{o} - \mathrm{o}^*)/(2\gamma_1) \tag{38}$$

where δ and γ_1 are positive constants and $\hat{\varepsilon}$ is the estimated value of the minimum reconstructed error ε. The estimation of the reconstructed error ε involves compensating for the observed error induced by the modified recurrent Laguerre OPNNUO and further guaranteeing the stable characteristics of the whole control system. The derivative of the Lyapunov function from (38) is obtained as

$$\begin{aligned} \dot{L}_3 &= \dot{L}_2 + (\hat{\varepsilon} - \varepsilon)\dot{\hat{\varepsilon}}/\delta + (\mathrm{o} - \mathrm{o}^*)^T \dot{\mathrm{o}}/\gamma_1 \\ &= -k_1 z_1^2 + z_2[-z_1 + a_1(z_2 + \eta) + b_1 u_a + q - \dot{\eta}] \\ &\quad + (\hat{\varepsilon} - \varepsilon)\dot{\hat{\varepsilon}}/\delta + (\mathrm{o} - \mathrm{o}^*)^T \dot{\mathrm{o}}/\gamma_1 \end{aligned} \tag{39}$$

According to (39), a backstepping control system using adaptive modified recurrent Laguerre OPNNUO $u_a = \hat{u}_a$ is proposed as follows:

$$u_a = \hat{u}_a = b_1^{-1}[z_1 - k_3 z_2 - a_1(z_2 + \eta) - \hat{\varepsilon} - \hat{q}(\mathrm{o}) + \dot{\eta}] \tag{40}$$

By substituting (40) into (39), the following equation can be obtained:

$$\begin{aligned} \dot{L}_3 &= -k_1 z_1^2 - k_3 z_2^2 + z_2 q - z_2 \hat{q} - z_2 \hat{\varepsilon} + \frac{1}{\delta}(\hat{\varepsilon} - \varepsilon)\dot{\hat{\varepsilon}} + \frac{1}{\gamma_1}(\mathrm{o} - \mathrm{o}^*)^T \dot{\mathrm{o}} \\ &= -k_1 z_1^2 - k_3 z_2^2 - z_2\hat{\varepsilon} + z_2(q - q(\mathrm{o}^*)) - z_2(\hat{q}(\mathrm{o}) - q(\mathrm{o}^*)) \\ &\quad + \frac{1}{\delta}(\hat{\varepsilon} - \varepsilon)\dot{\hat{\varepsilon}} + \frac{1}{\gamma_1}(\mathrm{o} - \mathrm{o}^*)^T \dot{\mathrm{o}} \\ &= -k_1 z_1^2 - k_3 z_2^2 - z_2(\hat{\varepsilon} - \varepsilon) - z_2(\mathrm{o} - \mathrm{o}^*)^T \psi \\ &\quad + \frac{1}{\delta}(\hat{\varepsilon} - \varepsilon)\dot{\hat{\varepsilon}} + \frac{1}{\gamma_1}(\mathrm{o} - \mathrm{o}^*)^T \dot{\mathrm{o}} \end{aligned} \tag{41}$$

The adaptive laws $\dot{\mathrm{o}}$ and $\dot{\hat{\varepsilon}}$ are designed as follows:

$$\dot{\mathrm{o}} = \gamma_1 z_2 \psi \tag{42}$$

$$\dot{\hat{\varepsilon}} = \delta z_2 \tag{43}$$

Thus, (41) can be rewritten as follows:

$$\dot{L}_3 = -k_1 z_1^2 - k_3 z_2^2 = \phi(t) \le 0 \tag{44}$$

By using Barbalat's lemma [14], [15], $\phi(t) \to 0$ as $t \to \infty$. That is, z_1 and z_2 converge to zero as $t \to \infty$. As a result, the stability of the proposed backstepping control system using an adaptive modified recurrent Laguerre OPNNUO (Fig. 3) can be guaranteed. Then again, the guaranteed convergence of the tracking error to zero does not imply the convergence of the estimated value of the lumped uncertainty to the real values. The persistent excitation condition [14], [15] should be satisfied for the estimated value to converge to its theoretical value.

According to the Lyapunov stability theorem and gradient descent method, an on-line parameter training methodology of the modified recurrent Laguerre OPNN can be derived and trained effectively. Then, the parameter of the adaptive law $\dot{\mathrm{o}}$ shown in (42) can be computed with the gradient descent method to select the appropriate learning rate. Parameter convergence can be guaranteed, but the convergence speed is relatively slow because of the low learning rate. By contrast, parameter convergence may oscillate because of a high learning rate. In efficiently training the modified recurrent Laguerre OPNN, two optimal learning rates are derived to achieve a rapid convergence of the output tracking error. The adaptation law $\dot{o}$ shown in (42) can then be rewritten as

$$\dot{w}_{kj}^{2} = \gamma_1 z_2 \Psi \quad (45)$$

To effectively train the parameters of the modified recurrent Laguerre OPNN, recursively obtaining a gradient vector is very important. Each component can be defined as the derivative of a cost function in the training algorithm. The gradient vector is calculated in the direction opposite to the flow of the output of each node by means of the chain rule. To describe the on-line training algorithm of the modified recurrent Laguerre OPNN, a cost function is defined as [10]

$$E_1 = z_2^2 / 2 \quad (46)$$

The adaptation law of the connective weight using the gradient descent method can be represented as

$$\dot{w}_{kj}^{2} = \gamma_1 z_2 \Psi \triangleq -\gamma_1 \frac{\partial E_1}{\partial y_k^3}\frac{\partial y_k^3}{\partial w_{kj}^2} = -\gamma_1 \frac{\partial E_1}{\partial y_k^3} y_j^2 \quad (47)$$

The above Jacobian term of the controlled system can be rewritten as $\partial E_1 / \partial y_k^3 = -z_2$. The recurrent weight w_{ik}^1 from the Jacobian term of the controlled system can be updated as

$$\dot{w}_{ik}^{1} \equiv -\gamma_2 \frac{\partial E_1}{\partial w_{ik}^1} = -\gamma_2 \frac{\partial E_1}{\partial y_k^3}\frac{\partial y_k^3}{\partial y_j^2}\frac{\partial y_j^2}{\partial y_i^1}\frac{\partial y_i^1}{\partial w_{ik}^1} = \gamma_2 z_2 w_{kj}^2 G_j P_i \quad (48)$$

where $P_i \equiv \partial y_i^1 / \partial w_{ik}^1$ can be calculated from (33). Then, two optimal learning rates are derived to ensure the convergence of the output tracking error. The convergence analysis is provided in the following two theorems.

Theorem 1: Assume that γ_1 is the learning rate of the connective weight between the hidden layer and the output layer in the modified recurrent Laguerre OPNN. Meanwhile, let Q_{1max} be defined as $Q_{1max} \equiv max_N \|Q_1(N)\|$, in which $Q_1(N) = \partial y_k^3 / \partial w_{kj}^2$ and $\|\cdot\|$ is the Euclidean norm in $\Re^n$. If γ_1 is chosen as [10, 11], then

$$0 < \gamma_1 < \frac{2}{(Q_{1\max})^2 [z_2 B_a / z_2(N)]^2} \quad (49)$$

The convergence of the output tracking error is guaranteed. Furthermore, the optimal learning rate, which achieves rapid convergence, can be obtained.

$$\gamma_1^* = 1/[(Q_{1\max})^2 [z_2 B_a / z_2(N)]^2] \quad (50)$$

Proof: Given that

$$Q_1(N) = \frac{\partial y_k^3}{\partial w_{kj}^2} = y_j^2 \quad (51)$$

Let a discrete-type Lyapunov function be selected as

$$L_4(N) = \frac{1}{2} z_2^2(N) \quad (52)$$

The change in the Lyapunov function is obtained by

$$\Delta L_4(N) = L_4(N+1) - L_4(N) = \frac{1}{2}\left[z_2^2(N+1) - z_2^2(N)\right] \quad (53)$$

Next, the error difference can be represented by

$$z_2(N+1) = z_2(N) + \Delta z_2(N) = z_2(N) + \left[\frac{\partial z_2(N)}{\partial w_{kj}^2}\right]^T \Delta w_{kj}^2 \quad (54)$$

in which $\Delta z_2(N)$ is the output error change and Δw_{kj}^2 represents the change in weight. Then, (54) can be obtained by means of (45), (46), (47), and (51).

$$\frac{\partial z_2(N)}{\partial w_{jk}^1} = \frac{\partial z_2(N)}{\partial E_1}\frac{\partial E_1}{\partial y_k^3}\frac{\partial y_k^3}{\partial w_{kj}^2} = -\frac{z_2 B_a}{z_2(N)} Q_1(N) \quad (55)$$

$$z_2(N+1) = z_2(N) - \left[\frac{z_2 B_a}{z_2(N)} Q_{1w}(N)\right]^T \gamma_1 z_2 B_a Q_1(N) \quad (56)$$

Therefore,

$$\begin{aligned} \|z_2(N+1)\| &= \left\| z_2(N)\left[1 - \gamma_1 (z_2 B_a / z_2(N))^2 Q_1^T(N) Q_1(N)\right]\right\| \\ &\le \|z_2(N)\| \left\| 1 - \gamma_1 (z_2 B_a / z_2(N))^2 Q_1^T(N) Q_1(N)\right\| \end{aligned} \quad (57)$$

By substituting (53) into (57), $\Delta L_4(N)$ can be rewritten as

$$\begin{aligned} \Delta L_4(N) &= \frac{1}{2}\gamma_1 \left[z_2 B_a\right]^2 Q_1^T(N) Q_1(N) \\ &\quad \cdot \left\{\gamma_1 \left[z_2 B_a / z_2(N)\right]^2 Q_1^T(N) Q_1(N) - 2\right\} \\ &\le \frac{1}{2}\gamma_1 \left[z_2 B_a\right]^2 (Q_{1\max}(N))^2 \\ &\quad \left\{\gamma_1 \left[z_2 B_a / z_2(N)\right]^2 (Q_{1\max}(N))^2 - 2\right\} \end{aligned} \quad (58)$$

If γ_1 is chosen as $0 < \gamma_1 < 2/\{(Q_{1\max})^2 [z_2 B_a / z_2(N)]^2\}$, then the Lyapunov stability of $L_4(N) > 0$ and $\Delta L_4 < 0$ is guaranteed. Then, the output tracking error converges to zero as $t \to 0$, which completes the proof of the theorem. Furthermore, the optimal learning rate, which achieves rapid convergence, corresponds to [16], [17]

$$2\gamma_1^* \{(Q_{1\max})^2 [z_2 B_a / z_2(N)]^2\} - 2 = 0 \quad (59)$$

i.e.,

$$\gamma_1^* = 1/\{(Q_{1\max})^2 [z_2 B_a / z_2(N)]^2\} = 1/\{(Q_{1\max})^2 (B_a)^2\} \quad (60)$$

which comes from the derivative of (58) with respect to γ_1 and equals zero. The results indicate the optimal learning rate can be tuned on-line instantly.

Theorem 2: Assume that γ_2 is the learning rate of the recurrent weight between the output layer and the input layer in the modified recurrent Laguerre OPNN. Meanwhile, let $Q_{2\max}$ be defined as $Q_{2\max} \equiv max_N \|Q_2(N)\|$, where

$Q_2(N)=\partial y_k^3/\partial w_{ik}^1$ and $\|\cdot\|$ is the Euclidean norm in $\Re^n$. If γ_2 is chosen as [10, 11], then

$$0<\gamma_2<\frac{2}{(Q_{2\max})^2[z_2B_a/z_2(N)]^2} \quad (61)$$

The convergence of the output tracking error is thereby guaranteed. Furthermore, the optimal learning rate, which achieves rapid convergence, can be obtained as

$$\gamma_2^*=1/[(Q_{2\max,})^2[z_2B_a/z_2(N)]^2] \quad (62)$$

Proof: Given that

$$Q_2(N)=\frac{\partial y_k^3}{\partial w_{ik}^1}=w_{kj}^2G_j(\cdot)x_i^1(N)y_k^3(N-1) \quad (63)$$

Let a discrete-type Lyapunov function be selected as (52), and let the change in the Lyapunov function be obtained with (53). Then, the error difference can be represented by

$$z_2(N+1)=z_2(N)+\Delta z_2(N)=z_2(N)+\left[\frac{\partial z_2(N)}{\partial w_{ik}^1}\right]^T\Delta w_{ik}^1 \quad (64)$$

where $\Delta z_2(N)$ is the output error change and Δw_{ik}^1 represents the change in weight. Then (64), by using (46), (48), and (63), can be represented as

$$\frac{\partial z_2(N)}{\partial w_{ik}^1}=\frac{\partial z_2(N)}{\partial E_1}\frac{\partial E_1}{\partial y_k^3}\frac{\partial y_k^3}{\partial w_{ik}^1}=-\frac{B_az_2}{z_2(N)}Q_2(N) \quad (65)$$

$$z_2(N+1)=z_2(N)-\left[\frac{B_az_2}{z_2(N)}Q_2(N)\right]^T\gamma_2B_az_2Q_2(N) \quad (66)$$

Therefore,

$$\begin{aligned}\|z_2(N+1)\|&=\left\|z_2(N)\left[1-\gamma_2\left(B_az_2/z_2(N)\right)^2Q_2^T(N)Q_2(N)\right]\right\|\\&\le\|z_2(N)\|\left\|1-\gamma_2\left(B_az_2/z_2(N)\right)^2Q_2^T(N)Q_2(N)\right\|\end{aligned} \quad (67)$$

By means of (53) and (64) to (67), $\Delta L_4(N)$ can be rewritten as

$$\begin{aligned}\Delta L_4(N)&=\frac{1}{2}\gamma_2\left[B_az_2\right]^2Q_2^T(N)Q_2(N)\\&\quad\left\{\gamma_2\left[B_az_2/z_2(N)\right]^2Q_2^T(N)Q_2(N)-2\right\}\\&\le\frac{1}{2}\gamma_2\left[B_az_2\right]^2\left(Q_{2\max}(N)\right)^2\\&\quad\left\{\gamma_2\left[B_az_2/z_2(N)\right]^2\left(Q_{2\max}(N)\right)^2-2\right\}\end{aligned} \quad (68)$$

If γ_2 is chosen as $0<\gamma_2<2/\{(Q_{2\max})^2[B_az_2/z_2(N)]^2\}$, then the Lyapunov stability of $L_4(N)>0$ and $\Delta L_4(N)<0$ is guaranteed such that the output tracking error converges to zero as $t\to 0$. At this point, the proof of the theorem is complete. Moreover, the optimal learning rate, which achieves rapid convergence, corresponds to [16], [17]

$$2\gamma_2^*\{(Q_{2\max})^2[B_az_2/z_2(N)]^2\}-2=0 \quad (69)$$

i.e.,

$$\gamma_2^*=1/\{(Q_{2\max})^2[B_az_2/z_2(N)]^2\}=1/\{(Q_{2\max})^2(B_a)^2\} \quad (70)$$

which comes from the derivative of (68) with respect to γ_2 and equals zero. This result shows that the optimal learning rate can be tuned on-line instantly.

In summary, the on-line tuning algorithm of the modified recurrent Laguerre OPNN is based on the adaptation laws (47) and (48) for the connective weight adjustment and recurrent weight adjustment with two optimal learning rates in (50) and (62), respectively. Moreover, the modified recurrent Legendre OPNN weight estimation errors are fundamentally bounded [18]. As long as the modified recurrent Laguerre OPNN weight estimation errors are bounded, the control signal is bounded.

IV. EXPERIMENTAL RESULTS

Experimental results are provided to demonstrate the control performance of the LSM drive system. A photo of the experimental setup is shown in Fig. 4. A host PC downloads the program running on DSP. The proposed controllers are implemented with the DSP control system. The current-controlled PWM VSI is implemented with the IGBT power modules with a switching frequency of 15 kHz. A DSP control board includes multi-channels of D/A and encoder interface circuits. The field-oriented mechanism drive system is implemented with the FPGA control system, and the control law is implemented with the DSP control system.

The parameters of the backstepping control system are $k_1=2.2$, $k_2=1.7$, and $k_3=2.3$ through some heuristic knowledge [20-22] resulting from the periodic step command from 0 mm to 84 mm at the nominal case for position tracking. In this way, good transient and steady-state control performance is achieved. The parameters of the backstepping control system using adaptive modified recurrent Laguerre OPNNUO are $k_1=2.2$, $k_2=1.7$, $k_3=2.3$, and $\delta=0.5$ according to heuristic knowledge [4-5] resulting from the periodic step command from 0 mm to 84 mm at the nominal case for position tracking. In this way, good transient and steady-state control performance is achieved. First, a second-order transfer function in the following form with a rise time of 0.1 s is chosen as the reference model [19] by using the reduction of order method for the periodical step command:

$$\left.\frac{d_r(s)}{d_m(s)}\right|_{f_L(s)=0}=\frac{1156}{s^2+68s+1156} \quad (71)$$

The control objective is to control the mover such that it

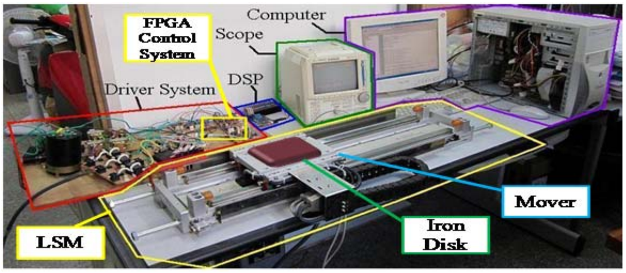

Fig. 4. Photo of the experimental setup.

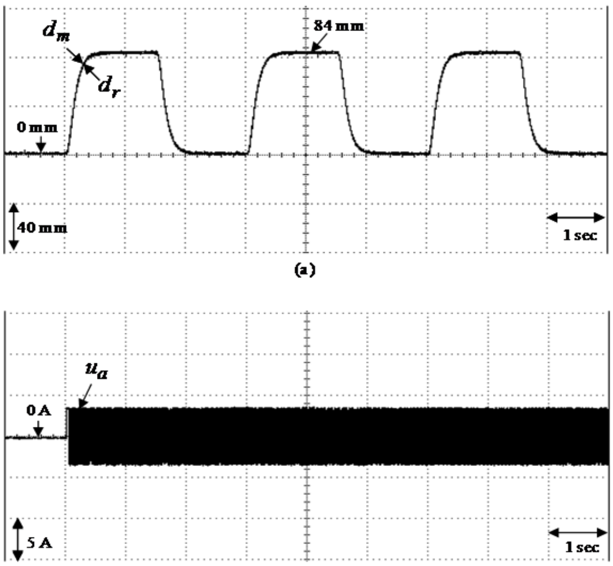

Fig. 5. Experimental results of the backstepping control system attributed to the periodic step command from 0 mm to 84 mm in the nominal case. (a) Position response of the mover. (b) Response of control effort.

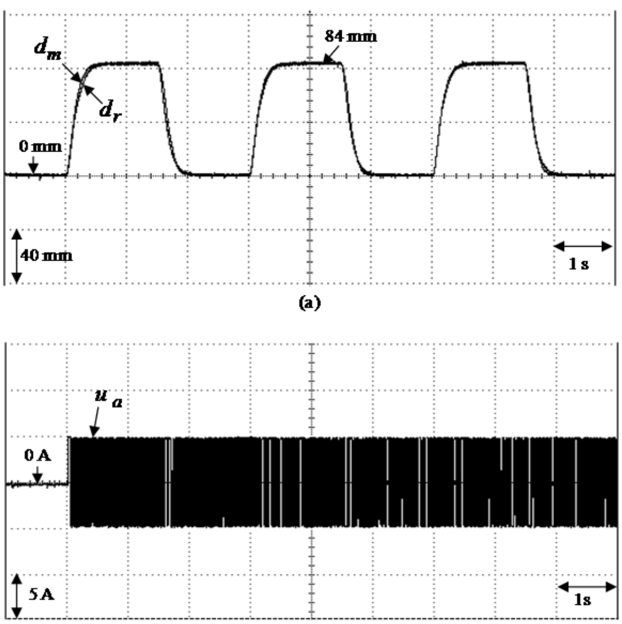

Fig. 6. Experimental results of the backstepping control system attributed to the periodic step command from 0 mm to 84 mm in the parameter disturbance case. (a) Position response of the mover. (b) Response of control effort.

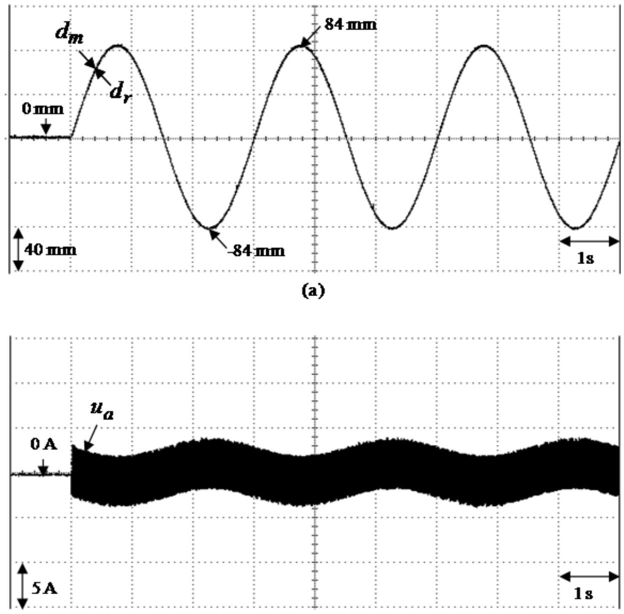

Fig. 7. Experimental results of the backstepping control system attributed to periodic sinusoidal command from –84 mm to 84 mm at the nominal case. (a) Position response of the mover. (b) Response of control effort.

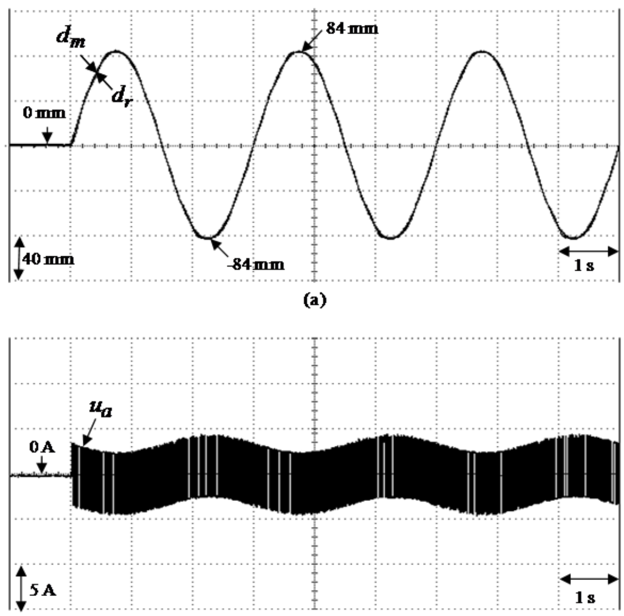

Fig. 8. Experimental results of backstepping control system attributed to the periodic sinusoidal command from −84 mm to 84 mm in the parameter disturbance case. (a) Position response of the mover. (b) Response of control effort.

moves 84 mm periodically. Then, when the command is a sinusoidal reference trajectory, the reference model is set as a unit gain. The sampling interval of the control processing in the experiment is set at 1 ms. To show the effectiveness of the control system with a small number of neurons, the modified recurrent Laguerre OPNN is equipped with two, four, and one neuron(s) in the input layer, hidden layer, and

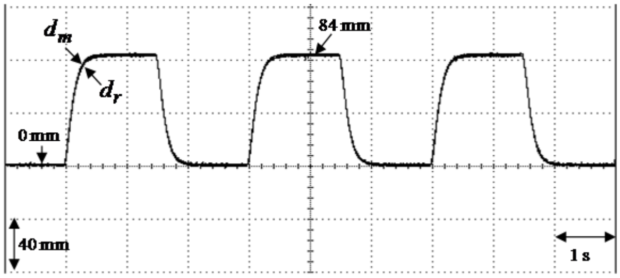

(a)

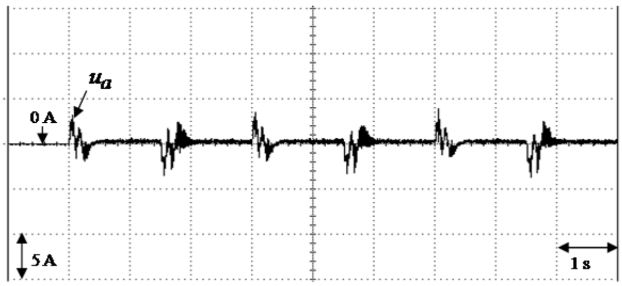

(b)

Fig. 9. Experimental results of the proposed backstepping control system using adaptive modified recurrent Laguerre OPNNUO attributed to the periodic step command from 0 mm to 84 mm in the nominal case. (a) Position response of the mover. (b) Response of control effort.

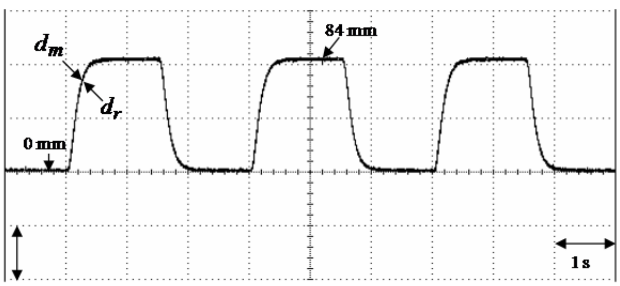

(a)

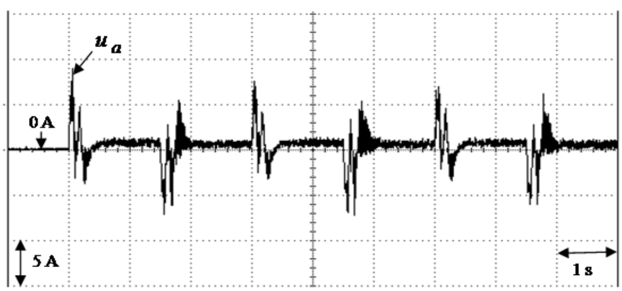

(b)

Fig. 10. Experimental results of the proposed backstepping control system using adaptive modified recurrent Laguerre OPNNUO attributed to the periodic step command from 0 mm to 84 mm in the parameter disturbance case. (a) Position response of the mover. (b) Response of control effort.

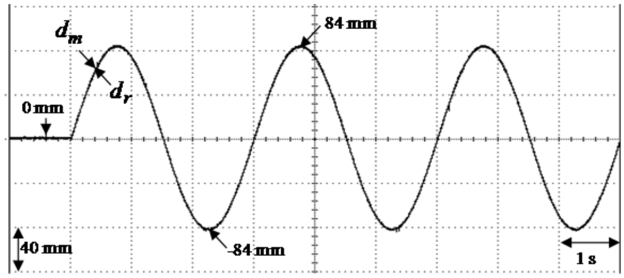

(a)

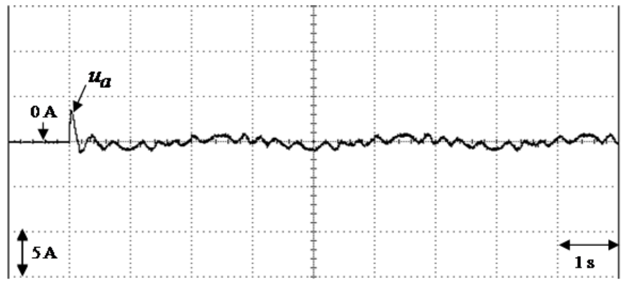

(b)

Fig. 11. Experimental results of the proposed backstepping control system using adaptive modified recurrent Laguerre OPNNUO attributed to the periodic sinusoidal command from −84 mm to 84 mm in the nominal case. (a) Position response of the mover. (b) Response of control effort.

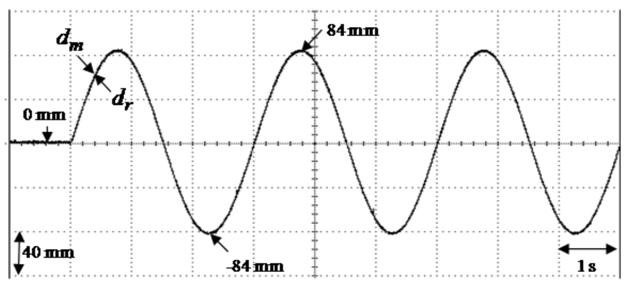

(a)

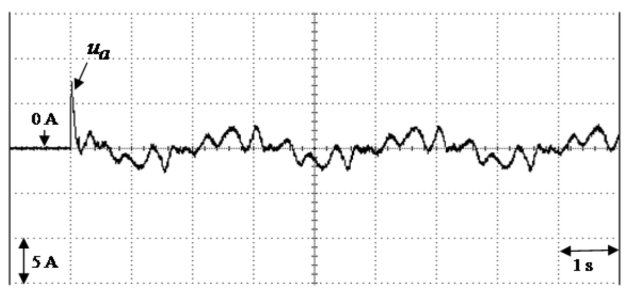

(b)

Fig. 12. Experimental results of the proposed backstepping control system using adaptive modified recurrent Laguerre OPNNUO attributed to the periodic sinusoidal command from −84 mm to 84 mm in the parameter disturbance case. (a) Position response of the mover. (b) Response of control effort.

output layer, respectively. The parameter adjustment process remains active for the duration of the experiment.

Some experimental results are provided to demonstrate the control performance of the proposed control system. Two test conditions are provided in the experiment: the nominal case and parameter variation case. The parameter variation case involves the addition of one 8.1 kg iron disk to the mass of the mover, i.e., the total mass is three times the nominal mass. The experimental results of the backstepping control system attributed to the periodic step command from 0 mm to 84 mm

TABLE I

CONTROL PERFORMANCE COMPARISON OF CONTROL SYSTEMS

Control System and Four Test Cases / Performance	Backstepping Control System			
	caused by periodic step command from 0 mm to 84 mm in the nominal case	caused by periodic step command from 0 mm to 84 mm in the parameter disturbance case	caused by periodic sinusoidal command from −84 mm to 84 mm in the nominal case	caused by periodic sinusoidal command from −84 mm to 84 mm in the parameter disturbance case
Maximum error of z_1	0.2 mm	1 mm	0.1 mm	0.3 mm
RMS error of z_1	0.05 mm	0. 25 mm	0.05 mm	0.15 mm
Control System and Four Test Cases / Performance	Backstepping Control System Using Adaptive Modified Recurrent Laguerre OPNNUO			
	caused by periodic step command from 0 mm to 84 mm in the nominal case	caused by periodic step command from 0 mm to 84 mm in the parameter disturbance case	caused by periodic sinusoidal command from −84 mm to 84 mm in the nominal case	caused by periodic sinusoidal command from −84 mm to 84 mm in the parameter disturbance case
Maximum error of z_1	0.2 mm	0.25 mm	0.1 mm	0.15 mm
RMS error of z_1	0.05 mm	0.05 mm	0.05 mm	0.05 mm

TABLE II

CHARACTERISTIC PERFORMANCE COMPARISON OF CONTROL SYSTEMS

Control System / Characteristic Performance	Backstepping Control System	Backstepping Control System Using Adaptive Modified Recurrent Laguerre OPNNUO
Dynamic response	Fast	Fast
Rejection of parameter disturbance	Good	Best
Convergence speed	Slow (tracking error response at 1 mm within 0.5 s)	Fast (tracking error response at 1 mm within 0.05 s) (varying learning Rate)
Load regulation capability	Good	Best
Learning rate	None	Varies (optimal learning rate)
Control effort	Large	Small
Chattering	Large	Small

in the nominal case and parameter variation case are shown in Figs. 5 and 6, respectively.

The position responses of the mover under the nominal case and parameter variation case are shown in Figs. 5(a) and 6(a), respectively, and the associated control efforts are shown in Figs. 5(b) and 6(b), respectively. The experimental results of the backstepping control system attributed to the periodic sinusoidal command from −84 mm to 84 mm in the nominal case and parameter variation case are shown in Figs. 7 and 8, respectively. The position responses of the mover under the nominal case and parameter variation case are shown in Figs. 7(a) and 8(a), respectively, and the associated control efforts are shown in Figs. 7(b), and 8(b), respectively. Although favorable tracking responses can be obtained by the backstepping control system, the chattering in the control efforts is critical because of the large control gain.

The experimental results of the proposed backstepping control system using adaptive modified recurrent Laguerre OPNNUO attributed to the periodic step command from 0 mm to 84 mm in the nominal case and parameter variation case are shown in Figs. 9 and 10, respectively.

The position responses of the mover in the nominal case and parameter variation case are shown in Figs. 9(a) and 10(a), respectively, and the associated control efforts are shown in Figs. 9(b) and 10(b), respectively. The experimental results of the proposed backstepping control system using adaptive modified recurrent Laguerre OPNNUO attributed to the periodic sinusoidal command from −84 mm to 84 mm in the nominal case and parameter variation case are shown in Figs. 11 and 12, respectively. The position responses of the mover in the nominal case and parameter variation case are shown in Figs. 11(a) and 12(a), respectively, and the associated control efforts are shown in Figs. 11(b) and 12(b), respectively.

However, the robust control performance of the proposed backstepping control system using adaptive modified recurrent Laguerre OPNNUO under the occurrence of parameter variation at different trajectories is obvious owing to the on-line adaptive adjustment of the modified recurrent Laguerre OPNN. As indicated by the experimental results, the control performance of the proposed backstepping control system using adaptive modified recurrent Laguerre OPNNUO is better than that of the backstepping control system for the tracking of periodic steps and sinusoidal commands.

The comparison of the control performances of the backstepping control system and the proposed backstepping control system using adaptive modified recurrent Laguerre OPNNUO with two optimal learning rates is summarized in Table I with respect to the experimental results of four test cases. As shown in the table, the proposed backstepping control system using adaptive modified recurrent Laguerre OPNNUO results in smaller tracking errors in comparison with the backstepping control system. According to the tabulated measurements, the proposed backstepping control system using adaptive modified recurrent Laguerre OPNNUO indeed yields superior control performance. The comparison of the characteristic performances of the backstepping control system and the proposed backstepping control system using adaptive modified recurrent Laguerre OPNNUO is summarized in Table II with respect to the experimental results. As shown in the table, the various performances of the proposed backstepping control system using adaptive modified recurrent Laguerre OPNNUO are superior to those of the backstepping control system.

V. CONCLUSION

A backstepping control system using adaptive modified recurrent Laguerre OPNNUO is proposed to control LSM drives for the tracking of periodic reference inputs. First, a field-oriented mechanism is applied to formulate the dynamic equation of the LSM servo drive. Then, the proposed backstepping control system using adaptive modified recurrent Laguerre OPNNUO is developed to control the LSM drive with parameter variations. With the backstepping control system, the mover position of the LSM drive achieves good transient control performance and robustness to uncertainties for the tracking of periodic reference trajectories. In increasing the robustness of the LSM drive, an adaptive modified recurrent Laguerre OPNNUO is proposed to estimate the required lumped uncertainty. The on-line parameter training methodology of the modified recurrent Laguerre OPNN is based on the Lyapunov stability theorem. Two optimal learning rates of the modified recurrent Laguerre OPNN are derived to accelerate parameter convergence. The effectiveness of the proposed control scheme is verified by experimental results.

ACKNOWLEDGMENT

The author would like to acknowledge the financial support of the Ministry of Science and Technology of Taiwan under grant MOST 104-2221-E-239 -011.

REFERENCES

[1] I. Boldea and S. A. Nasar, *Linear Electric Actuators and Generators,* London: Cambridge University Press, 1997.

[2] T. Egami and T. Tsuchiya, "Disturbance suppression control with preview action of linear DC brushless motor," *IEEE Trans. Ind. Electron.*, Vol. 42, No. 5, pp. 494-500, Oct. 1995.

[3] M. Sanada, S. Morimoto, and Y. Takeda, "Interior permanent magnet linear synchronous motor for high-performance drives," *IEEE Trans. Ind. Appl.*, Vol. 33, No. 5, pp. 966-972, Jul./Aug. 1997.

[4] I. Kanellakopoulos, P. V. Kokotovic, and A. S. Morse, "Systematic design of adaptive controller for feedback linearizable system," *IEEE Trans. Autom. Contr.,* Vol. 36, No. 11, pp. 1241-1253, Nov. 1991.

[5] G. Bartolini, A. Ferrara, L. Giacomini, and E. Usai, "Peoperties of a combined adaptive/second-order sliding mode control algorithm for some classes of uncertain nonlinear systems," *IEEE Trans. Autom. Contr.*, Vol. 45, No. 7, pp. 1334-1341, Jul. 2000.

[6] M. N. Eskander, "Minimization of losses in permanent magnet synchronous motors using neural network," *Journal of Power Electronics,* Vol. 2, No. 3, pp 220-229, Jul. 2002.

[7] A. F. Payam, M. N. Hashemnia, and J. Faiz, "Robust DTC control of doubly-fed induction machines based on input-output feedback linearization using recurrent neural networks," *Journal of Power Electronics,* Vol. 11, No. 5, pp. 719-725, Sep. 2011.

[8] C. H. Lin, "A PMSM driven electric scooter system with V-belt continuously variable transmission using novel hybrid modified recurrent Legendre neural network control," *Journal of Power Electronics*, Vol. 14, No. 5, pp 220-229, Sep. 2014.

[9] C. H. Lin, "Novel adaptive recurrent Legendre neural network control for PMSM servo-drive electric scooter," *J. Dynamic Systems, Measurement, and Control- Transactions of the ASME*, Vol. 137 / 011010-1, 12 pages, 2015.

[10] C. H. Lin, "Dynamic control of V-belt continuously variable transmission-driven electric scooter using hybrid modified recurrent Legendre neural network control system," *Nonlinear Dynamics*, Vol. 79, No. 2, pp. 787-808, 2015.

[11] C. H. Lin, "Hybrid recurrent Laguerre-orthogonal-polynomial NN control system applied in V-belt continuously variable transmission system using particle swarm optimization," *Mathematical Problems in Engineering*, Vol. 2015, Article ID 106707, 17 pages, 2015.

[12] J. C. Patra, C. Bornand and P. K. Meher, "Laguerre neural network-based smart sensors for wireless sensor networks," *IEEE Instrumentation and Measurement Technology Conference*, pp. 832-837, 2009.

[13] J. C. Patra, P. K. Meher, and G. Chakraborty, "Development of Laguerre neural-network-based intelligent sensors for wireless sensor networks," *IEEE Trans. Instrum. Meas.*, Vol. 60, No. 3, pp. 725-734, Mar.2011.

[14] J. J. E. Slotine and W. Li, *Applied Nonlinear Control*, Englewood Cliffs, NJ: Prentice-Hall, 1991.

[15] J. Astrom and B. Wittenmark, *Adaptive Control*, New York: Addison-Wesley, 1995.

[16] C. C. Ku and K. Y. Lee, "Diagonal recurrent neural networks for dynamic system control," *IEEE Trans. Neural Netw.*, Vol. 6, No. 1, pp.144-156, Jan. 1995.

[17] C. H. Lin, "Recurrent modified Elman neural network control of PM synchronous generator system using wind turbine emulator of PM synchronous servo motor drive," *Intl. J. Electrical Power and Energy Systems*, Vol. 52, pp. 143-160, Nov. 2013.

[18] F. L. Lewis, J. Campos and R. Selmic, *Neuro-Fuzzy Control of Industrial Systems with Actuator Nonlinearities.* SIAM Frontiers in Applied Mathematics, 2002.

[19] F. J. Lin and C. H. Lin, "On-line gain-tuning IP controller using RFNN," *IEEE Trans. Aerosp. Electron. Syst.*, Vol. 37, No. 2, pp. 655-670, Apr. 2001.

[20] K. J. Astrom and T. Hagglund, *PID Controller: Theory, Design, and Tuning,* North Carolina: Instrument Society of America, Research Triangle Park, 1995

[21] T. Hagglund and K. J. Astrom, "Revisiting the Ziegler-Nichols tuning rules for PI control," *Asian J. Control,* Vol. 4, No. 4, pp. 364-380, Dec. 2002.

[22] T. Hagglund and K. J. Astrom, "Revisiting the Ziegler-Nichols tuning rules for PI control – Part II: The frequency response method," *Asian J. Control,* Vol. 6, No. 4, pp. 469-482, Dec. 2004.

Chih-Hong Lin was born in Taichung, Taiwan, R.O.C. He received his B.S. and M.S. degrees in Electrical Engineering from the National Taiwan University of Science and Technology, Taipei, Taiwan, R.O.C., in 1989 and 1991, respectively. He received his Ph.D. degree in Electrical Engineering from Chung Yuan Christian University, Chung Li, Taiwan, R.O.C., in 2001. He is currently an Associate Professor in the Department of Electrical Engineering, National United University, Miao Li, Taiwan, R.O.C. His current research interests include power electronics, motor servo drives, and intelligent control.